

# Mitigating Shuttle Effect in Lithium–Sulfur Batteries by Separators

Subjects: [Materials Science](#), [Coatings & Films](#)

Contributor: Yingbao Zhu , Zhou Chen , Hui Chen , Xuguang Fu , Desire Emefa Awuye , Xichen Yin , Yixuan Zhao

Lithium–sulfur (Li-S) batteries are considered one of the most promising energy storage systems due to their high theoretical capacity, high theoretical capacity density, and low cost. However, challenges such as poor conductivity of sulfur (S) elements in active materials, the “shuttle effect” caused by lithium polysulfide, and the growth of lithium dendrites impede the commercial development of Li-S batteries. As a crucial component of the battery, the separator plays a vital role in mitigating the shuttle effect caused by polysulfide. Traditional polypropylene, polyethylene, and polyimide separators are constrained by their inherent limitations, rendering them unsuitable for direct application in lithium–sulfur batteries. Therefore, there is an urgent need for the development of novel separators.

lithium–sulfur batteries

shuttle effect

separator

separator modification

## 1. Introduction

With the rising demand for electric vehicles and portable electronic devices, it is important to research and develop energy storage systems with high energy density, low cost, and extended service life <sup>[1]</sup>. Traditional lithium batteries are widely used due to their high working voltage, long cycle life, and good stability <sup>[2]</sup>. However, the high production cost, theoretical specific capacity, and low energy density of the electrode material make it difficult for traditional lithium batteries to meet the increasing market scale <sup>[3]</sup>. Lithium-sulfur (Li-S) batteries are regarded as one of the energy storage systems with great potential due to its low production cost, high theoretical specific capacity and energy density, abundant S elements in nature, and low toxicity <sup>[4]</sup>. They are also facing great challenges, such as the poor conductivity of S elements, the volume expansion of the cathode material, and the shuttle effect caused by lithium polysulfide in the commercial development of Li-S <sup>[5][6]</sup>. Solving the above problems is crucial for the commercialization of lithium-sulfur batteries.

Li-S batteries are composed of an anode, a cathode, an electrolyte, and a separator, as shown in **Figure 1**, which represents a schematic diagram of a typical Li-S battery, in which the separator plays a key role in solving the shuttle effect of lithium polysulfide <sup>[7][8]</sup>. The shuttle effect occurs because lithium polysulfide is easily soluble in the electrolyte and moves between the cathode and the anode, resulting in irreversible volume loss <sup>[9]</sup>. Therefore, studying a separator with excellent performance is very important in order to solve the shuttle effect.

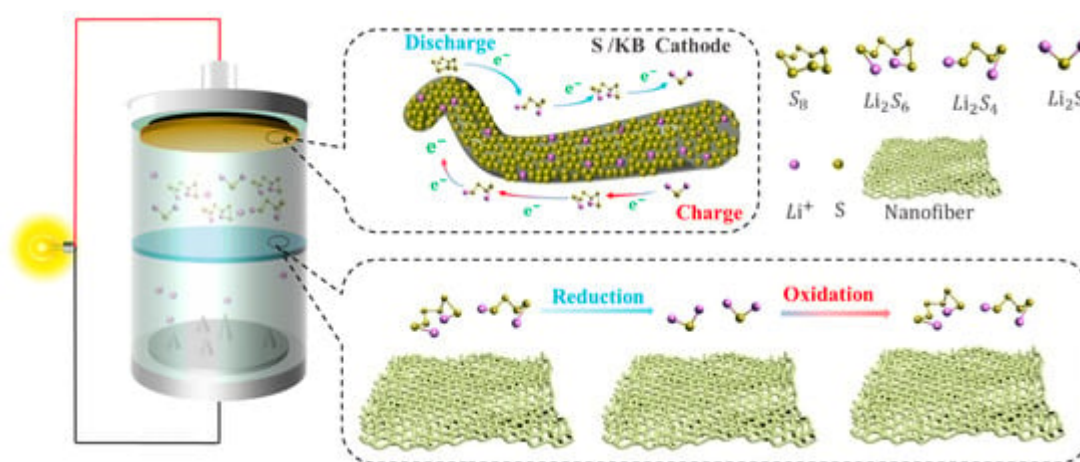


Figure 1. Lithium–sulfur battery model separator.

## 2. The Working Principle and Problems of Li-S

### 2.1. Working Mechanism of Li-S

The electrochemical reactions that occur in Li-S are different from traditional lithium batteries [10], and the redox reaction during the charging and discharging of Li-S involves the conversion between different valence ions of the S atom, making it more complex than traditional lithium-ion batteries [11][12]. Lithium–sulfur batteries generally consist of a lithium metal negative electrode, an organic liquid electrolyte, and a sulfur–carbon composite positive electrode [13]. Taking a positive electrode material such as sulfur elemental as an example, during discharge, the lithium metal of the anode is oxidized to generate electrons and lithium ions, and the lithium ions diffuse to the cathode through the electrolyte. At the same time, the electrons move to the sulfur element of the cathode through the external circuit, the sulfur element is reduced to  $S^{2-}$ , and  $S^{2-}$  and  $Li^+$  generate  $Li_2S$  at the cathode [14]. During the discharge process, when the sulfur element in the cathode reacts completely with the lithium ion, the total equation of the electrochemical reaction is as follows:



As shown in **Figure 2a**, the spatial structure of elemental sulfur is formed by eight sulfur atoms connected by covalent bonding, so there are multiple cleavage and bonding sites of S-S bonds in sulfur elements, resulting in more complex redox reactions in the charging and discharging process of Li-S [13][15]. At present, there are many studies on the S conversion of lithium–sulfur battery charging and discharging process [15][16]. According to the measurement of the electrolyte mass spectrometry (LC/MS) of different charges and discharges, the reduction reaction of elemental sulfur is carried out in multiple steps, and there are a variety of different intermediate products, such as  $Li_2S_8$ ,  $Li_2S_6$ ,  $Li_2S_4$ ,  $Li_2S_2$ , and  $Li_2S$  [17].

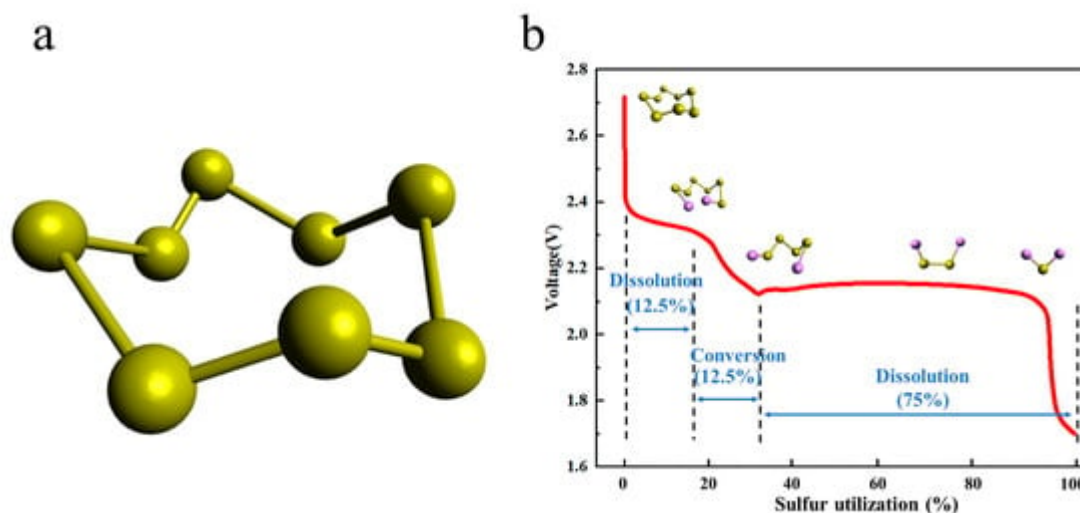


**Figure 2.** (a) Schematic diagram of the spatial structure of elemental sulfur. (b) Red is the discharge curve of lithium-sulfur battery, showing the sulfur electrode utilization.

When discharging, the electrochemical reaction is as formulated (2)–(6) [10]:



As can be seen in **Figure 2b**, it can be seen from the discharge curve of the Li-S that there are two discharge platforms in the discharge process [18]. The high discharge platform is between 2.3–2.4 V; at this time, the S<sub>8</sub> product is a variety of soluble long-chain lithium polysulfide Li<sub>2</sub>S<sub>x</sub> (4 ≤ x ≤ 8) [19]. The low discharge platform is between 1.8–2.1 V; at this time, the corresponding long-chain lithium polysulfide Li<sub>2</sub>S<sub>x</sub> (4 ≤ x ≤ 8) is further reduced to short-chain lithium polysulfide Li<sub>2</sub>S<sub>x</sub> (1 ≤ x ≤ 4) [20] (Wu et al. [21]). According to experimental calculations, the

utilization rate of the active material of the high discharge platform is only 25%, and the theoretical capacity of the process is 418 mAh g<sup>-1</sup>. The active material utilization rate of the low discharge platform is 75%, and the theoretical capacity of the process is 1254 mAh g<sup>-1</sup>. At the low discharge platform, due to the growth of lithium dendrites and phase transition processes, the reaction kinetics of this process slow down, and the actual discharge-specific capacity of the battery is lower than the theoretical capacity, so the actual specific capacity of the Li-S is lower than the theoretical specific capacity throughout the entire discharge process [22][23][24][25].

When charging, there is only one noticeable platform of about 2.4 V [26]. Electrochemical reactions can be described by Formulas (7) and (8):



## 2.2. The Existing Problems of Li-S

### 2.2.1. Cathode

Because sulfur resources are abundant, non-toxic, and non-polluting; the theoretical specific capacity is 1675 mAh g<sup>-1</sup>; and they have low prices and other advantages, sulfur was selected as the cathode material in Li-S batteries [27][28][29]. However, problems such as low conductivity, volume expansion during electrochemical reactions, and shuttle effect lead to low coulombic efficiency, and the actual specific capacity is much lower than the theoretical specific capacity, in addition to poor cycle stability [30].

### 2.2.2. Separator

As a vital part of Li-S, separators play a great role in the performance of Li-S [31]. During the charging and discharging process of lithium–sulfur batteries, the separator does not directly participate in the electrochemical reaction of mutual conversion between polysulfides [32]. However, the wettability, thermal stability, mechanical properties, porosity, liquid absorption rate, and other properties of the separator affect the specific capacity and cycle life of the Li-S. As a separator for Li-S, it is not only necessary to maintain the advantages of wettability, thermal stability, mechanical properties, porosity, and liquid absorption rate [33], but also to effectively suppress the shuttle effect [34].

### 2.2.3. Anode

The weight density is low, and the theoretical specific capacity is 3860 mAh g<sup>-1</sup> higher [35]. Due to its low reduction potential [36][37] and other advantages, lithium metal was chosen as the electrode material for Li-S. Metallic lithium

is used as an anode in Li-S [38] due to the growth of lithium dendrites [39][40][41][42]. Lithium dendrites easily pierce the separator, resulting in potential safety hazards in the circuit. Lithium metal itself has strong activity and can easily have side reactions with electrolytes, resulting in low battery cycle life and other problems that limit the commercial development of Li-S.

#### 2.2.4. Electrolyte

Electrolytes, as a pivotal constituent bridging the positive and negative electrodes, wield substantial influence on the transport of lithium ions, thereby exerting a direct impact on the performance of lithium–sulfur batteries. Electrolytes can be classified into two categories: liquid electrolytes and solid electrolytes.

Presently, liquid electrolytes find extensive application in lithium–sulfur batteries, primarily owing to their facile synthesis, high ionic conductivity, and favorable chemical stability. Nevertheless, liquid electrolytes are not without their challenges. Firstly, at the positive electrode, liquid electrolytes tend to dissolve polysulfides, which subsequently diffuse through the electrolyte to the negative electrode, leading to diminished Coulombic efficiency and corrosion of the lithium negative electrode. Secondly, liquid electrolytes typically comprise flammable organic solvents, thus posing safety concerns when exposed to elevated temperatures. In response to these issues associated with liquid electrolytes, a substantial body of researchers is actively engaged in addressing these challenges. This includes the modification of electrolyte composition, the exploration of novel multi-component solvents, and the incorporation of functional additives [43].

#### 2.2.5. Binders

Binders, constituting an integral part of the sulfur cathode in lithium–sulfur batteries, serve the crucial function of ensuring effective electrochemical contact among the conductive agent, sulfur, and current collector. Moreover, they mitigate volumetric variations of active materials during cycling. Binders play a pivotal role in lithium–sulfur batteries, and the commonly utilized types encompass polymeric, bio-based, and inorganic binders. Challenges regarding binders encompass inadequate mechanical properties and the detachment of electrode materials during cycling, consequently leading to a diminished cycling lifespan and reduced stability of the battery.

#### 2.2.6. Current Collector

Aluminum foil has found widespread application as a current collector for sulfur cathodes. However, at elevated temperatures, aluminum and sulfur can undergo reactions, which may pose safety concerns. Presently, the use of carbon-coated aluminum foil is employed to mitigate direct contact between sulfur and aluminum foil, thereby enhancing the safety of lithium–sulfur batteries. The presence of carbon coatings effectively improves the adhesion between the active materials and the current collector, while simultaneously enhancing electrical conductivity [44] (Figure 3).

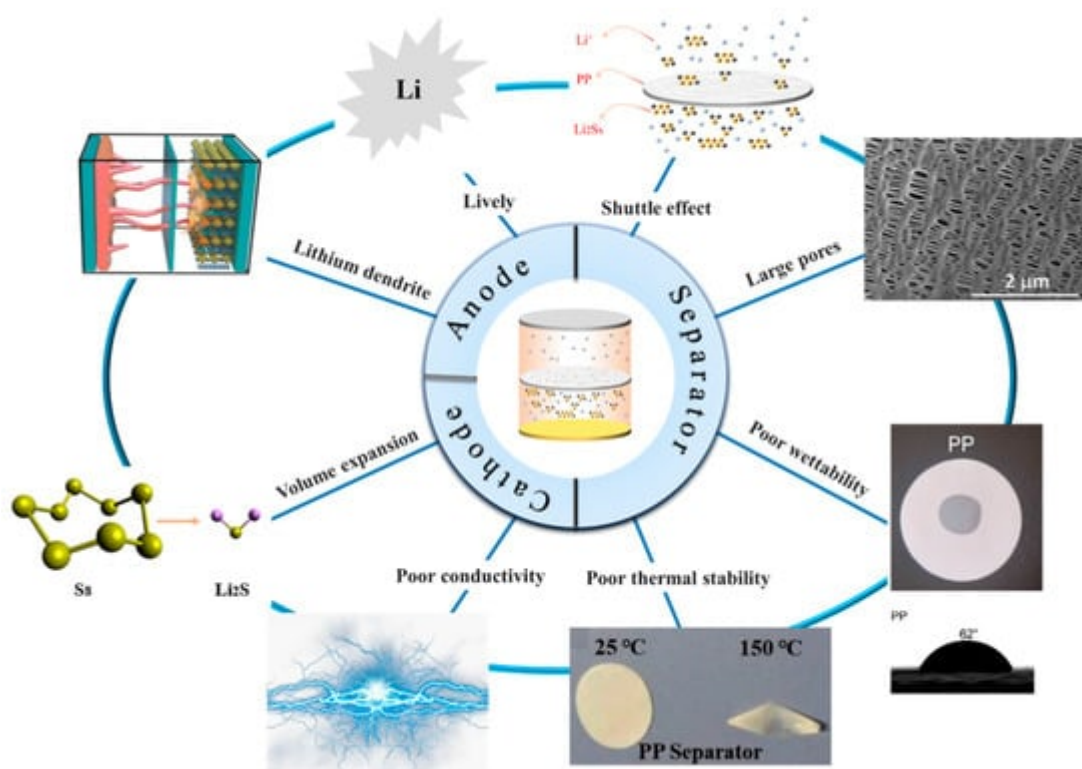


**Figure 3.** Existing problems with lithium–sulfur batteries [45]. Reproduced with permission from the Polymers.

## 3. Methods

With the development of science and technology, separator technology has also been continuously developed and updated, and the methods of preparing polymer separators have also been diversified. Different preparation methods can be selected according to the material properties and separator application direction. The battery separator film is closely related to the energy density, stability, and cycle life of the battery [46]. A battery separator composed of nanofibers has the advantages of a large specific area and high porosity [47], which has attracted close attention. There are many methods of separators, but electrospinning [48], vacuum filtration [49], wet spinning [50], the coating method [51][52], the in situ growth method [53], and atomic layer deposition [54] are more commonly used to prepare separators.

### 3.1. Electrospinning

Electrospinning is a novel technique for preparing nanofiber separators, the principle of which is as follows:: under the action of a high-voltage electrostatic field, the polymer forms a Taylor cone when it flows out of the needle, and a continuously charged jet is ejected and deposited on the collector as nonwoven nanofibers [55]. The nanofibers prepared by electrospinning can reach the nanometer diameter [48][56], and the prepared nanofiber separator has the advantages of high porosity, large specific surface area, and small pore size [57]. As shown in **Figure 4**, electrospinning technology has prepared a variety of nanostructured fibers. The electrospinning method has received great attention in the field of battery separators in recent years.

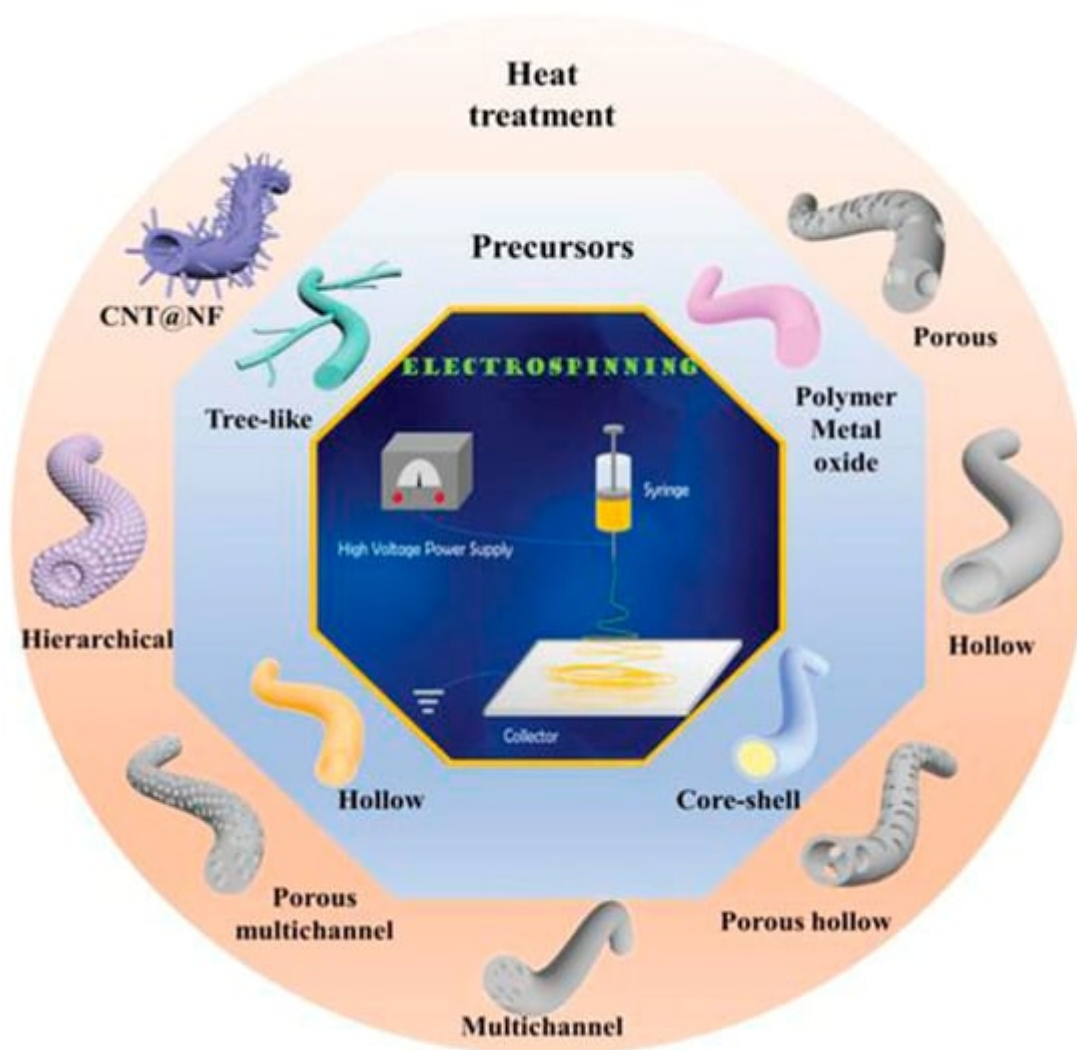


**Figure 4.** The electrospinning technology has prepared a variety of nanostructured fibers [2]. Reproduced with permission from the Advanced Functional Materials.

### 3.2. Vacuum Filtration

The vacuum filtration method is a new method for preparing separators using the interfacial composite method, which has the advantages of convenient operation, a simple process, and no specific process equipment. Its working principle is that the film-forming material is uniformly dispersed in the solvent, and then under vacuum filtration conditions, the film-forming material is deposited on the substrate due to the flow function of solvent molecules. The disadvantage is that due to the limitations of process conditions, the structure of the produced nanofibers is uncontrollable and unsuitable for large-scale mass production [58].

### 3.3. Wet Spinning

The nanofiber non-woven separator prepared by the wet laying method has high porosity and good affinity with electrolytes [59]. The principle is that different polymer fibers are used to separate matrix fibers and adhesive fibers, which are continuously randomly laid on the screen belt after mixing in a water-soluble suspension, sent to a

ventilation drying box to heat and soften the bonded fibers, and then calendered by a heating drum to obtain a non-woven film [46]. The disadvantages are that the structure and properties of the nanofibers prepared by this method are limited by the type and composition of the polymer in the suspension, and the operation is more complicated [60].

### 3.4. Coating Method

The coating method is one of the most commonly used modification methods. A layer of modified material is coated on one side of the separator by means of physical methods, and polysulfides are adsorbed by the modified material to improve the shortcomings of the separator. Because the coating method is simple to operate, relatively low in cost, can be used for large-area separator modification, and is suitable for industrial production, the coating method is widely used in the modification of lithium–sulfur battery separators. However, the coating method has problems such as difficulty in accurately controlling the thickness of the separator. The viscosity of the material has an impact on the coating effect, and some polymer materials are not suitable for the preparation of the coating method.

### 3.5. In Situ Growth Method

The in situ growth method is a relatively novel method of separator modification. Compared with other modification methods, this method can effectively generate a lightweight barrier on one side of the separator and avoid excessive thickness of the separator; in addition, the in situ growth method can achieve efficient use of materials, thereby reducing costs. However, the current in situ growth method is still in the experimental research stage. In addition, the modification process is relatively complicated, and it is difficult to achieve mass production.

### 3.6. Atomic Layer Deposition (ALD)

Atomic layer deposition is a method in which substances can be plated on the surface of the substrate, layer by layer, in the form of a single-atom film. It has similarities to chemical vapor deposition [61]. Its working principle is a method in which a gas precursor pulse alternately enters the reactor and chemically adsorbs and reacts on the deposition matrix to form a deposition film. A typical ALD cycle consists of two self-limiting semi-reactions [62], and it is this reaction property that allows the separator's thickness to be precisely controlled. However, the atomic layer deposition method has disadvantages such as high requirements for reaction conditions, a complicated production process, expensive equipment, and a slow deposition rate.

## 4. Application of Separators in Lithium–Sulfur Batteries

### 4.1. Electrospinning

#### 4.1.1. Separator

In Li-S, the separator is required to suppress the shuttle effect, good electrolyte wettability, and good ionic conductivity [63]. Nanofiber separators prepared using the electrospinning technique exhibit extremely fine fibers, with exceptionally high specific surface areas. Additionally, these separators possess a notably high level of porosity, a feature inherent to their unique fabrication process. Owing to their elevated specific surface areas and porosity, such separators can provide a greater quantity of electrolytes during the charge and discharge processes of lithium–sulfur batteries. This augmentation of reaction sites enhances electrochemical reactions. In recent years, numerous researchers have achieved significant advancements by incorporating modified materials onto the fiber surface, aiming to adsorb polysulfides and mitigate the shuttle effect, thereby improving the cyclic lifespan and practical specific capacity of the batteries (Guo et al. [64]).

#### 4.1.2. Interlayer

A highly conductive electrospun nanofiber interlayer is introduced between the positive electrode and the separator to effectively improve the performance of lithium–sulfur batteries. Electrospun carbon nanofibers, owing to their excellent electrical conductivity, serve to reduce internal resistance within batteries, thus enhancing the rates of electron and ion transport. Additionally, carbon nanofibers exhibit Van Der Waals interactions with polysulfides, facilitating their adsorption. Guo et al. [65] utilized electrospinning technology to prepare a  $\text{Ti}_4\text{O}_7/\text{C}$  nanofiber (TCNF) interlayer. The incorporation of carbon nanofibers in this interlayer offered several advantages, including a large specific surface area and high electrical conductivity, which significantly enhanced the conversion and electron transfer of polysulfides. Additionally,  $\text{Ti}_4\text{O}_7$  formed strong chemical bonds with polysulfides, effectively mitigating their shuttle effect.

### 4.2. Vacuum Filtration

#### 4.2.1. Separator

According to Yigeng et al. [66], They modified the PP separator through suction filtration, a depositing a layer of g-C<sub>3</sub>N<sub>4</sub> composite on one side of it. It had abundant adsorption sites and contributed to the solidification of polysulfides. The process of polysulfide solidification entails immobilizing polysulfide species onto the cathode material or the cathode-proximate regions of the separator. This strategic immobilization serves as an effective countermeasure against the undesirable migration of polysulfides towards the anode, thereby mitigating capacity fade and consequentially augmenting the performance characteristics of lithium–sulfur batteries.

#### 4.2.2. Interlayer

Feng et al. [67] prepared a 2D NiCo MOF/CNT as the middle layer of a lithium–sulfur battery and filtered it onto PP through vacuum filtration. The thickness of 2D NiCo MOF/CNT was only a few nanometers, and the CNT built a conductive network to enhance electronic conductivity while serving as a physical barrier to prevent polysulfide migration. The 2D NiCo MOF/CNT improved the catalytic performance due to abundant and accessible active sites. The lithium–sulfur battery using 2D NiCo MOF/CNT interlayer had an initial discharge-specific capacity of 1132.7 mAh g<sup>-1</sup> at 0.5 C, and it maintained 709.1 mAh/g<sup>-1</sup> after 300 cycles, showing good cycle stability and rate performance.

### 4.3. Wet Spinning

Currently, commercial PP and PE separators are prepared using a wet process. However, when used directly in lithium–sulfur batteries, the PP separator leads to a significant shuttle effect, resulting in a sharp decrease in the specific discharge capacity of the battery. Main applications include functional interlayers in Li-S [11][68][69][70][71] and electrodes [72][73]. Li et al. [69] successfully prepared a carbon paper sandwich via a wet process with excellent electrical conductivity of  $11.9 \text{ S cm}^{-1}$ . A high initial capacity, up to  $1091 \text{ mAh g}^{-1}$ , was achieved when using carbon paper as an interlayer for Li-S. At 5 C,  $631 \text{ mAh g}^{-1}$  was maintained after 200 cycles (0.21% capacity decay per cycle).

### 4.4. Coating Method

#### 4.4.1. Separator

Polar metal oxide titanium dioxide ( $\text{TiO}_2$ ) exhibits a strong chemical interaction with polysulfides, making it widely applicable in the field of lithium–sulfur batteries. This is attributed to the ability of oxygen atoms on the surface of  $\text{TiO}_2$  to form chemical bonds with sulfur atoms present in polysulfides, facilitating the effective adsorption of polysulfides. Additionally, the high electronegativity of the  $\text{TiO}_2$  surface enables it to counteract the shuttle effect of polysulfides through a charge repulsion mechanism. Gao et al. [74] coated the PP separator with a layer of titanium dioxide, modified multi-walled carbon nanotube composites ( $\text{TiO}_2@\text{SCNT}/\text{PP}$  separator), and applied the separator to Li-S, and the data showed that the performance of the separator and the pre-modification period greatly improved.

#### 4.4.2. Interlayer

Wang et al. [75] prepared the NC-Co interlayer using a coating method. The intermediate layer effectively inhibited the shuttling of polysulfides. At 1 C, the first discharge-specific capacity of the lithium–sulfur battery using the interlayer was  $1216.9 \text{ mAh g}^{-1}$ , and it maintained  $660.3 \text{ mAh g}^{-1}$  after 250 cycles. The Coulombic efficiency remained above 99% during the cycle. After 100 cycles, the surface SEM of the negative lithium metal showed that the lithium negative electrode with the interlayer had few surface cracks, while the lithium metal without the interlayer had obvious cracks, indicating that the use of the interlayer can significantly inhibit the corrosion of the negative metal lithium.

### 4.5. In Situ Growth Method

#### 4.5.1. Separator

Lu et al. [76] modified a PP separator via in situ growth. On the side of the PP separator, a layer of polar hydrated sulfate  $\text{CoSO}_4 \cdot 4\text{H}_2\text{O}$  material (CS/PP separator) was grown in situ, and the cobalt sulfate hydrate had strong polarity and catalytic properties, which can effectively adsorb polysulfides. In the preparation flow chart, it can be seen by scanning electron microscopy that the surface of the separator was attached to a layer similar to the shape of a sea urchin, the single sea urchin was assembled from the nanoneedles of several microns, and the separator

exhibited good mechanical stability. The data show that when the material reaction time was 6 h, the separator showed the best performance, which was denoted as CS/PP-6. At 1 C, the initial specific capacity of the modified separator reached as high as 807.7 mAh g<sup>-1</sup>. After 500 cycles, it still maintained 504.6 mAh g<sup>-1</sup> (compared to 208.7 mAh g<sup>-1</sup> for the PP separator), and the Coulombic efficiency reached as high as 97%. When the discharge current was restored to 0.1 C, the reversible capacity was 1308.6 mAh g<sup>-1</sup>, indicating that the lithium–sulfur battery using the separator had good reversibility and good electrochemical performance.

#### 4.5.2. Interlayer

Li et al. [77] prepared the ZIF/CNFs interlayer via the situ growth method. The interlayer had an obvious effect of inhibiting polysulfide shuttling. According to SEM and TEM images, ZIF-64 particles were distributed on the fiber, and due to the special binding site of ZIF-64, it inhibited the shuttling of polysulfides during circulation. At 1 C, it exhibited a high discharge-specific capacity of 1334 mAh/g, which remained at 569 mAh/g after 300 cycles.

### 4.6. Atomic Layer Deposition

#### 4.6.1. Separator

At present, owing to the distinctive attributes of the Atomic Layer Deposition (ALD) fabrication process, there is a scarcity of literature that directly employs ALD for the modification of polypropylene (PP) separators. Usually, people use methods such as cooperating with other preparation processes (coating, suction filtration, etc.) to modify the separator.

#### 4.6.2. Interlayer

Lin et al. [54] prepared the CNT@SACo interlayer by atomic layer deposition and applied it to lithium–sulfur batteries. From the experimental results, the CNT@SACo interlayer exhibits catalytic activity catalyzes the conversion of polysulfides, and inhibits the shuttling of polysulfides. The lithium–sulfur battery with the CNT@SACo interlayer exhibited a high discharge specific capacity of 880 mAh/g at 1 C, and maintained a capacity of 595 mAh/g after 500 cycles, with a capacity decay rate of 0.064% per cycle.

## 5. Conclusions

In recent years, with the rising demand for new energy, it has become important to develop an energy storage system with high energy density, low cost, and a long cycle life. Traditional lithium batteries have a high cost and low energy density, which makes it difficult for them to meet the huge market demand. Li-S batteries are regarded as one of the most promising energy storage systems due to their high theoretical specific capacity and low cost. Li-S batteries also have some urgent problems to solve, such as poor conductivity of S, the expansion of the positive electrode volume during the electrochemical reaction, and the most important problem, the shuttle effect caused by polysulfides. As an important component of lithium–sulfur batteries, separators are very important in suppressing the shuttle effect of polysulfides.

## References

1. Kang, N.; Lin, Y.X.; Yang, L.; Lu, D.P.; Xiao, J.; Qi, Y.; Cai, M. Cathode porosity is a missing key parameter to optimize lithium-sulfur battery energy density. *Nat. Commun.* 2019, 10, 4597.
2. Liu, M.; Deng, N.P.; Ju, J.G.; Fan, L.L.; Wang, L.Y.; Li, Z.J.; Zhao, H.J.; Yang, G.; Kang, W.M.; Yan, J.; et al. A Review: Electrospun Nanofiber Materials for Lithium-Sulfur Batteries. *Adv. Funct. Mater.* 2019, 29, 1905467.
3. Din, M.M.U.; Murugan, R. Metal Coated Polypropylene Separator with Enhanced Surface Wettability for High Capacity Lithium Metal Batteries. *Sci. Rep.* 2019, 9, 16795.
4. Jeong, Y.C.; Kim, J.H.; Nam, S.; Park, C.R.; Yang, S.J. Rational Design of Nanostructured Functional Interlayer/Separator for Advanced Li-S Batteries. *Adv. Funct. Mater.* 2018, 28, 1707411.
5. Cuisinier, M.; Hart, C.; Balasubramanian, M.; Garsuch, A.; Nazar, L.F. Radical or Not Radical: Revisiting Lithium-Sulfur Electrochemistry in Nonaqueous Electrolytes. *Adv. Energy Mater.* 2015, 5, 1401801.
6. Yuan, Z.; Peng, H.J.; Hou, T.Z.; Huang, J.Q.; Chen, C.M.; Wang, D.W.; Cheng, X.B.; Wei, F.; Zhang, Q. Powering Lithium-Sulfur Battery Performance by Propelling Polysulfide Redox at Sulfiphilic Hosts. *Nano Lett.* 2016, 16, 519–527.
7. Song, Y.Z.; Cai, W.L.; Kong, L.; Cai, J.S.; Zhang, Q.; Sun, J.Y. Rationalizing Electrocatalysis of Li-S Chemistry by Mediator Design: Progress and Prospects. *Adv. Energy Mater.* 2020, 10, 1901075.
8. Ren, W.C.; Ma, W.; Zhang, S.F.; Tang, B.T. Recent advances in shuttle effect inhibition for lithium sulfur batteries. *Energy Storage Mater.* 2019, 23, 707–732.
9. Liu, H.; Lai, W.-H.; Yang, H.-L.; Zhu, Y.-F.; Lei, Y.-J.; Zhao, L.; Peng, J.; Wang, Y.-X.; Chou, S.-L.; Liu, H.-K. Efficient separators with fast Li-ion transfer and high polysulfide entrapment for superior lithium-sulfur batteries. *Chem. Eng. J.* 2021, 408, 127348.
10. Phung, J.; Zhang, X.Z.; Deng, W.J.; Li, G. An overview of MOF-based separators for lithium-sulfur batteries. *Sustain. Mater. Technol.* 2022, 31, e00374.
11. Zhang, Y.S.; Zhang, X.L.; Silva, S.R.P.; Ding, B.; Zhang, P.; Shao, G.S. Lithium-Sulfur Batteries Meet Electrospinning: Recent Advances and the Key Parameters for High Gravimetric and Volume Energy Density. *Adv. Sci.* 2022, 9, 2103879.
12. Zhang, Y.G.; Yang, S.; Zhou, S.Y.; Zhang, L.B.; Gu, B.B.; Dong, Y.Y.; Kong, S.Z.; Cai, D.; Fang, G.Y.; Nie, H.G.; et al. Oxygen doping in antimony sulfide nanosheets to facilitate catalytic

- conversion of polysulfides for lithium-sulfur batteries. *Chem. Commun.* 2021, 57, 3255–3258.
13. Manthiram, A.; Fu, Y.; Su, Y.-S. Challenges and Prospects of Lithium–Sulfur Batteries. *Acc. Chem. Res.* 2013, 46, 1125–1134.
  14. Cuisinier, M.; Cabelguen, P.E.; Evers, S.; He, G.; Kolbeck, M.; Garsuch, A.; Bolin, T.; Balasubramanian, M.; Nazar, L.F. Sulfur Speciation in Li-S Batteries Determined by Operando X-ray Absorption Spectroscopy. *J. Phys. Chem. Lett.* 2013, 4, 3227–3232.
  15. Diao, Y.; Xie, K.; Xiong, S.; Hong, X. Analysis of Polysulfide Dissolved in Electrolyte in Discharge-Charge Process of Li-S Battery. *J. Electrochem. Soc.* 2012, 159, A421–A425.
  16. Wild, M.; O'Neill, L.; Zhang, T.; Purkayastha, R.; Minton, G.; Marinescu, M.; Offer, G.J. Lithium sulfur batteries, a mechanistic review. *Energy Environ. Sci.* 2015, 8, 3477–3494.
  17. Zhao, E.Y.; Nie, K.H.; Yu, X.Q.; Hu, Y.S.; Wang, F.W.; Xiao, J.; Li, H.; Huang, X.J. Advanced Characterization Techniques in Promoting Mechanism Understanding for Lithium-Sulfur Batteries. *Adv. Funct. Mater.* 2018, 28, 1707543.
  18. Sun, J.; Sun, Y.M.; Pasta, M.; Zhou, G.M.; Li, Y.Z.; Liu, W.; Xiong, F.; Cui, Y. Entrapment of Polysulfides by a Black-Phosphorus-Modified Separator for Lithium-Sulfur Batteries. *Adv. Mater.* 2016, 28, 9797–9803.
  19. Yao, S.S.; Cui, J.; Huang, J.Q.; Lu, Z.H.; Deng, Y.; Chong, W.G.; Wu, J.X.; Ihsan Ul Haq, M.; Ciucci, F.; Kim, J.K. Novel 2D Sb<sub>2</sub>S<sub>3</sub> Nanosheet/CNT Coupling Layer for Exceptional Polysulfide Recycling Performance. *Adv. Energy Mater.* 2018, 8, 1800710.
  20. Park, J.; Kim, E.T.; Kim, C.; Pyun, J.; Jang, H.S.; Shin, J.; Choi, J.W.; Char, K.; Sung, Y.E. The Importance of Confined Sulfur Nanodomains and Adjoining Electron Conductive Pathways in Subreaction Regimes of Li-S Batteries. *Adv. Energy Mater.* 2017, 7, 1700074.
  21. Wu, J.Y.; Zeng, H.X.; Li, X.W.; Pei, H.J.; Xue, Z.G.; Ye, Y.S.; Xie, X.L. Dual-Functional Interlayer Based on Radially Oriented Ultrathin MoS<sub>2</sub> Nanosheets for High-Performance Lithium Sulfur-Batteries. *Acs Appl. Energy Mater.* 2019, 2, 1702–1711.
  22. Zhao, M.; Li, B.-Q.; Chen, X.; Xie, J.; Yuan, H.; Huang, J.-Q. Redox Comediation with Organopolysulfides in Working Lithium-Sulfur Batteries. *Chem* 2020, 6, 3297–3311.
  23. Zhao, M.; Peng, Y.-Q.; Li, B.-Q.; Zhang, X.-Q.; Huang, J.-Q. Regulation of carbon distribution to construct high-sulfur-content cathode in lithium–sulfur batteries. *J. Energy Chem.* 2021, 56, 203–208.
  24. Sadd, M.; De Angelis, S.; Colding-Jorgensen, S.; Blanchard, D.; Johnsen, R.E.; Sanna, S.; Borisova, E.; Matic, A.; Bowen, J.R. Visualization of Dissolution-Precipitation Processes in Lithium-Sulfur Batteries. *Adv. Energy Mater.* 2022, 12, 2103126.

25. Ren, Y.X.; Zhao, T.S.; Liu, M.; Tan, P.; Zeng, Y.K. Modeling of lithium-sulfur batteries incorporating the effect of Li<sub>2</sub>S precipitation. *J. Power Sources* 2016, 336, 115–125.
26. Jayaprakash, N.; Shen, J.; Moganty, S.S.; Corona, A.; Archer, L.A. Porous Hollow Carbon@Sulfur Composites for High-Power Lithium-Sulfur Batteries. *Angew. Chem. Int. Ed.* 2011, 50, 5904–5908.
27. Guo, J.; Yang, Z.; Yu, Y.; Abruna, H.D.; Archer, L.A. Lithium-sulfur battery cathode enabled by lithium-nitrile interaction. *J. Am. Chem. Soc.* 2013, 135, 763–767.
28. Wang, H.; Yang, Y.; Liang, Y.; Robinson, J.T.; Li, Y.; Jackson, A.; Cui, Y.; Dai, H. Graphene-wrapped sulfur particles as a rechargeable lithium-sulfur battery cathode material with high capacity and cycling stability. *Nano Lett.* 2011, 11, 2644–2647.
29. Barai, P.; Mistry, A.; Mukherjee, P.P. Poromechanical effect in the lithium–sulfur battery cathode. *Extrem. Mech. Lett.* 2016, 9, 359–370.
30. Yan, J.H.; Liu, X.B.; Li, B.Y. Capacity Fade Analysis of Sulfur Cathodes in Lithium-Sulfur Batteries. *Adv. Sci.* 2016, 3, 1600101.
31. Ghazi, Z.A.; He, X.; Khattak, A.M.; Khan, N.A.; Liang, B.; Iqbal, A.; Wang, J.X.; Sin, H.S.; Li, L.S.; Tang, Z.Y. MoS<sub>2</sub>/Celgard Separator as Efficient Polysulfide Barrier for Long-Life Lithium-Sulfur Batteries. *Adv. Mater.* 2017, 29, 1606817.
32. Zhai, P.; Liu, K.; Wang, Z.; Shi, L.; Yuan, S. Multifunctional separators for high-performance lithium-ion batteries. *J. Power Sources* 2021, 499, 229973.
33. Lei, T.; Chen, W.; Lv, W.; Huang, J.; Zhu, J.; Chu, J.; Yan, C.; Wu, C.; Yan, Y.; He, W.; et al. Inhibiting Polysulfide Shuttling with a Graphene Composite Separator for Highly Robust Lithium-Sulfur Batteries. *Joule* 2018, 2, 2091–2104.
34. Gao, Z.; Xue, Z.; Miao, Y.; Chen, B.; Xu, J.; Shi, H.; Tang, T.; Zhao, X. TiO<sub>2</sub>@Porous carbon nanotubes modified separator as polysulfide barrier for lithium-sulfur batteries. *J. Alloys Compd.* 2022, 906, 164249.
35. Cao, R.; Xu, W.; Lv, D.; Xiao, J.; Zhang, J.-G. Anodes for Rechargeable Lithium-Sulfur Batteries. *Adv. Energy Mater.* 2015, 5, 1402273.
36. Cheng, X.B.; Huang, J.Q.; Zhang, Q. Review-Li Metal Anode in Working Lithium-Sulfur Batteries. *J. Electrochem. Soc.* 2018, 165, A6058–A6072.
37. Xiong, S.; Xie, K.; Diao, Y.; Hong, X. Characterization of the solid electrolyte interphase on lithium anode for preventing the shuttle mechanism in lithium–sulfur batteries. *J. Power Sources* 2014, 246, 840–845.
38. Rong, G.L.; Zhang, X.Y.; Zhao, W.; Qiu, Y.C.; Liu, M.N.; Ye, F.M.; Xu, Y.; Chen, J.F.; Hou, Y.; Li, W.F.; et al. Liquid-Phase Electrochemical Scanning Electron Microscopy for In Situ Investigation

- of Lithium Dendrite Growth and Dissolution. *Adv. Mater.* 2017, 29, 1606187.
39. Wang, J.; Yi, S.; Liu, J.; Sun, S.; Liu, Y.; Yang, D.; Xi, K.; Gao, G.; Abdelkader, A.; Yan, W.; et al. Suppressing the Shuttle Effect and Dendrite Growth in Lithium-Sulfur Batteries. *ACS Nano* 2020, 14, 9819–9831.
  40. Rosso, M.; Brissot, C.; Teyssot, A.; Dolle, M.; Sannier, L.; Tarascon, J.M.; Bouchet, R.; Lascaud, S. Dendrite short-circuit and fuse effect on Li/polymer/Li cells. *Electrochim. Acta* 2006, 51, 5334–5340.
  41. Fan, L.; Chen, S.H.; Zhu, J.Y.; Ma, R.F.; Li, S.P.; Podila, R.; Rao, A.M.; Yang, G.Z.; Wang, C.X.; Liu, Q.; et al. Simultaneous Suppression of the Dendrite Formation and Shuttle Effect in a Lithium-Sulfur Battery by Bilateral Solid Electrolyte Interface. *Adv. Sci.* 2018, 5, 1700934.
  42. Hu, Y.; Chen, W.; Lei, T.; Jiao, Y.; Wang, H.; Wang, X.; Rao, G.; Wang, X.; Chen, B.; Xiong, J. Graphene quantum dots as the nucleation sites and interfacial regulator to suppress lithium dendrites for high-loading lithium-sulfur battery. *Nano Energy* 2020, 68, 104373.
  43. Wang, L.; Liu, J.; Yuan, S.; Wang, Y.; Xia, Y. To mitigate self-discharge of lithium–sulfur batteries by optimizing ionic liquid electrolytes. *Energy Environ. Sci.* 2016, 9, 224–231.
  44. Zhang, S.S. Liquid electrolyte lithium/sulfur battery: Fundamental chemistry, problems, and solutions. *J. Power Sources* 2013, 231, 153–162.
  45. Li, Y.; Wang, X.; Liang, J.; Wu, K.; Xu, L.; Wang, J. Design of a high performance zeolite/polyimide composite separator for lithium-ion batteries. *Polymers* 2020, 12, 764.
  46. Li, Y.; Li, Q.; Tan, Z. A review of electrospun nanofiber-based separators for rechargeable lithium-ion batteries. *J. Power Sources* 2019, 443, 227262.
  47. Zhao, M.; Wang, J.; Chong, C.B.; Yu, X.W.; Wang, L.L.; Shi, Z.Q. An electrospun lignin/polyacrylonitrile nonwoven composite separator with high porosity and thermal stability for lithium-ion batteries. *RSC Adv.* 2015, 5, 101115–101120.
  48. Rutledge, G.C.; Fridrikh, S.V. Formation of fibers by electrospinning. *Adv. Drug Deliv. Rev.* 2007, 59, 1384–1391.
  49. Gao, W.L.; Kono, J. Science and applications of wafer-scale crystalline carbon nanotube films prepared through controlled vacuum filtration. *R. Soc. Open Sci.* 2019, 6, 181605.
  50. Kritzer, P. Nonwoven support material for improved separators in Li–polymer batteries. *J. Power Sources* 2006, 161, 1335–1340.
  51. Zhu, J.; Ge, Y.; Kim, D.; Lu, Y.; Chen, C.; Jiang, M.; Zhang, X. A novel separator coated by carbon for achieving exceptional high performance lithium-sulfur batteries. *Nano Energy* 2016, 20, 176–184.

52. Shao, H.; Wang, W.; Zhang, H.; Wang, A.; Chen, X.; Huang, Y. Nano-TiO<sub>2</sub> decorated carbon coating on the separator to physically and chemically suppress the shuttle effect for lithium-sulfur battery. *J. Power Sources* 2018, 378, 537–545.
53. Yang, L.W.; Wang, Y.; Li, Q.; Li, Y.; Chen, Y.X.; Liu, Y.X.; Wu, Z.G.; Wang, G.K.; Zhong, B.H.; Song, Y.; et al. Inhibition of the shuttle effect of lithium-sulfur batteries via a tannic acid-metal one-step in situ chemical film-forming modified separator. *Nanoscale* 2021, 13, 5058–5068.
54. Lin, Q.Y.; Ding, B.; Chen, S.; Li, P.; Li, Z.W.; Shi, Y.Y.; Dou, H.; Zhang, X.G. Atomic Layer Deposition of Single Atomic Cobalt as a Catalytic Interlayer for Lithium-Sulfur Batteries. *ACS Appl. Energy Mater.* 2020, 3, 11206–11212.
55. Bhardwaj, N.; Kundu, S.C. Electrospinning: A fascinating fiber fabrication technique. *Biotechnol. Adv.* 2010, 28, 325–347.
56. Demir, M.M.; Yilgor, I.; Yilgor, E.; Erman, B. Electrospinning of polyurethane fibers. *Polymer* 2002, 43, 3303–3309.
57. Hao, J.; Lei, G.; Li, Z.; Wu, L.; Xiao, Q.; Wang, L. A novel polyethylene terephthalate nonwoven separator based on electrospinning technique for lithium ion battery. *J. Membr. Sci.* 2013, 428, 11–16.
58. Zhang, L.Y.; Batchelor, W.; Varanasi, S.; Tsuzuki, T.; Wang, X.G. Effect of cellulose nanofiber dimensions on sheet forming through filtration. *Cellulose* 2012, 19, 561–574.
59. Cho, T.-H.; Tanaka, M.; Ohnishi, H.; Kondo, Y.; Yoshikazu, M.; Nakamura, T.; Sakai, T. Composite nonwoven separator for lithium-ion battery: Development and characterization. *J. Power Sources* 2010, 195, 4272–4277.
60. Safavi, A.; Fathi, S.; Babaei, M.R.; Mansoori, Z.; Latifi, M. Experimental and numerical analysis of fiber characteristics effects on fiber dispersion for wet-laid nonwoven. *Fibers Polym.* 2009, 10, 231–236.
61. Wang, X.R.; Yushin, G. Chemical vapor deposition and atomic layer deposition for advanced lithium ion batteries and supercapacitors. *Energy Environ. Sci.* 2015, 8, 1889–1904.
62. Yan, B.; Li, X.; Bai, Z.; Song, X.; Xiong, D.; Zhao, M.; Li, D.; Lu, S. A review of atomic layer deposition providing high performance lithium sulfur batteries. *J. Power Sources* 2017, 338, 34–48.
63. Zhu, X.B.; Ouyang, Y.; Chen, J.W.; Zhu, X.G.; Luo, X.; Lai, F.L.; Zhang, H.; Miao, Y.E.; Liu, T.X. In situ extracted poly(acrylic acid) contributing to electrospun nanofiber separators with precisely tuned pore structures for ultra-stable lithium-sulfur batteries. *J. Mater. Chem. A* 2019, 7, 3253–3263.

64. Guo, P.; Jiang, P.; Chen, W.; Qian, G.; He, D.; Lu, X. Bifunctional Al<sub>2</sub>O<sub>3</sub>/polyacrylonitrile membrane to suppress the growth of lithium dendrites and shuttling of polysulfides in lithium-sulfur batteries. *Electrochim. Acta* 2022, 428, 140955.
65. Guo, Y.; Li, J.; Pitcheri, R.; Zhu, J.; Wen, P.; Qiu, Y. Electrospun Ti<sub>4</sub>O<sub>7</sub>/C conductive nanofibers as interlayer for lithium-sulfur batteries with ultra long cycle life and high-rate capability. *Chem. Eng. J.* 2019, 355, 390–398.
66. Huangfu, Y.; Zheng, T.; Zhang, K.; She, X.; Xu, H.; Fang, Z.; Xie, K. Facile fabrication of permselective g-C<sub>3</sub>N<sub>4</sub> separator for improved lithium-sulfur batteries. *Electrochim. Acta* 2018, 272, 60–67.
67. Feng, P.; Hou, W.; Bai, Z.; Bai, Y.; Sun, K.; Wang, Z. Ultrathin two-dimensional bimetal NiCo-based MOF nanosheets as ultralight interlayer in lithium-sulfur batteries. *Chin. Chem. Lett.* 2023, 34, 107427.
68. Meng, L.; Li, Y.; Lin, Q.X.; Long, J.; Wang, Y.; Hu, J. Nitrogen and Oxygen Dual Self-Doped Flexible PPTA Nanofiber Carbon Paper as an Effective Interlayer for Lithium-Sulfur Batteries. *ACS Appl. Energy Mater.* 2021, 4, 8592–8603.
69. Li, Y.; Meng, L.; Jin, L.; Yun, L.; Jian, H. A wet-laid carbon paper with 3D conductive structure as an interlayer for lithium-sulfur batteries. *Mater. Res. Express* 2019, 6, 125547.
70. Chong, W.G.; Xiao, F.; Yao, S.S.; Cui, J.; Sadighi, Z.; Wu, J.X.; Ihsan-UI-Haq, M.; Shao, M.H.; Kim, J.K. Nitrogen-doped graphene fiber webs for multi-battery energy storage. *Nanoscale* 2019, 11, 6334–6342.
71. Suriyakumar, S.; Stephan, A.M. Mitigation of Polysulfide Shuttling by Interlayer/Permselective Separators in Lithium-Sulfur Batteries. *ACS Appl. Energy Mater.* 2020, 3, 8095–8129.
72. Chong, W.G.; Huang, J.Q.; Xu, Z.L.; Qin, X.Y.; Wang, X.Y.; Kim, J.K. Lithium-Sulfur Battery Cable Made from Ultralight, Flexible Graphene/Carbon Nanotube/Sulfur Composite Fibers. *Adv. Funct. Mater.* 2017, 27, 1604815.
73. Chong, W.G.; Xiao, Y.; Huang, J.-Q.; Yao, S.; Cui, J.; Qin, L.; Gao, C.; Kim, J.-K. Highly conductive porous graphene/sulfur composite ribbon electrodes for flexible lithium-sulfur batteries. *Nanoscale* 2018, 10, 21132–21141.
74. Bruckner, J.; Thieme, S.; Bottger-Hiller, F.; Bauer, I.; Grossmann, H.T.; Strubel, P.; Althues, H.; Spange, S.; Kaskel, S. Carbon- Based Anodes for Lithium Sulfur Full Cells with High Cycle Stability. *Adv. Funct. Mater.* 2014, 24, 1284–1289.
75. Wang, J.; Wu, T.; Zhang, S.; Gu, S.; Jin, J.; Wen, Z. Metal-organic-framework-derived N-C-Co film as a shuttle-suppressing interlayer for lithium sulfur battery. *Chem. Eng. J.* 2018, 334, 2356–2362.

76. Lu, X.; Wang, H.; Liu, X.; Song, Z.; Jiang, N.; Xie, F.; Zheng, Q.; Lin, D. Functional separators prepared via in-situ growth of hollow CoSO<sub>4</sub> hydrate arrays on pristine polypropylene membrane for high performance lithium-Sulfur batteries. *J. Alloys Compd.* 2020, 838, 155618.
77. Li, J.; Jiao, C.; Zhu, J.; Zhong, L.; Kang, T.; Aslam, S.; Wang, J.; Zhao, S.; Qiu, Y. Hybrid co-based MOF nanoboxes/CNFs interlayer as microreactors for polysulfides-trapping in lithium-sulfur batteries. *J. Energy Chem.* 2021, 57, 469–476.
- 

Retrieved from <https://encyclopedia.pub/entry/history/show/119440>